COSMIC RAYS ABOVE 0.1 EeV -RESULTS FROM THE FLY'S EYE EXPERIMENT

Presented by P. Sokolsky

D.J. Bird,[1] S.C. Corbató,[3] H.Y. Dai,[3] B.R. Dawson,[2]
J.W. Elbert,[3] T.K. Gaisser,[4] M.H.A. Huang,[3] D.B. Kieda,[3] S. Ko,[3]
C.G. Larsen,[3] E.C. Loh,[3] M.H. Salamon,[3]
J.D. Smith,[3] P. Sokolsky,[3] P. Sommers,[3] T. Stanev,[4] S. Tilav,[4] J.K.K. Tang [3] and S.B. Thomas [3]
[1] *Department of Physics, University of Illinois at Urbana-Champaign, Urbana, IL 61801 USA*
[2] *Department of Physics and Mathematical Physics, University of Adelaide, Adelaide, South Australia 5001 Australia*
[3] *High Energy Astrophysics Institute,Department of Physics, University of Utah, Salt Lake City UT 84112 USA*
[4] *Bartol Research Institute, University of Delaware, Newark DE 19716*

ABSTRACT

We present recent results from the Fly's Eye experiment. The results from the F.E. I and F.E. II stereo detectors indicate structure in the cosmic ray spectrum above 10^{18} eV. The composition of cosmic rays is found to change from a predominantly heavy composition near 10^{17} eV to a predominantly light one near 10^{19} eV. The spectral structure and changing composition can be accounted for by a simple two-component model. Higher statistics but lower resolution data from the F.E. I detector alone shows the presence of an outstanding 320 EeV energy event.

1. INTRODUCTION

The Fly's Eye experiment has been taking data since 1981 [Baltrusaitis et al. 1985]. A second fly's eye, F.E. II was built in 1986. This second eye views a significant fraction of events that trigger F.E. I. Such events have two independent views and are thus easily reconstructed. In addition to much improved geometrical reconstruction of the EAS trajectory, these events have two independent measurements of their energy and the position of shower maximum in the atmosphere (X_{max}). Such redundant measurements allow us to study the detector resolution in energy and X_{max}. Understanding detector resolution is crucial if structure in spectra are to be believable. Combining the measurements also results in a more accurate value for these variables. We report on results on the cosmic ray spectrum and composition for stereo data taken from 11/86 to 7/92 and monocular data taken since 1/82.

2. DATA ANALYSIS AND RESOLUTION

The air shower reconstruction process falls into two major divisions: geometric reconstruction and shower profile reconstruction. When a shower is seen simultaneously by Fly's Eye I and II, a shower-detector plane for each detector can be determined and the intersection of these planes defines the shower trajectory. If a shower is seen by only one detector, a fit to the relative arrival times of the signals is done and the shower trajectory determined. Given the track geometry, the EAS longitudinal size $N_e(x)$ is calculated via an iterative process to remove the contributions due to direct and scattered Cherenkov radiation. The residual photo-electrons (after the Cherenkov contribution is removed and various attenuation effects between source and detector are taken into account) result from the atmospheric scintillation process and therefore are directly proportional to the charged particle size within a tube's field of view. Each resultant longitudinal shower profile is approximated by a Gaussian function and the total primary energy and X_{max} are found from the fitted parameters.

We compare the energy calculated independently by F.E. I and F.E. II for events registered by both eyes. If E_1 is the energy measured by F.E. I and E_2 is the energy measured by F.E. II, the systematic shift between F.E. I and F.E. II is 2.5%. The distribution in the variable $(E_1 - E_2/E_{average}$ has a standard deviation of 0.47 for events below $2 \cdot 10^{18}$ eV and 0.40 for events above. The resulting stereo energy resolutions are 24% and 20% respectively. The systematic error in energy is dominated by the scintillation efficiency uncertainty of 20%.

The resolution in the variable X_{max} is found in the same way. The result is consistent with a resolution of 45 gm/cm^2. Uncertainties in the makeup of the atmosphere and residual Chrenkov light produce a systematic error in X_{max} of 20 gm/cm^2.

3. SPECTRUM

Fig. 1 shows the stereo energy spectrum derived from the number of events observed and the calculated stereo exposure [Bird et al. 1993a]. It is clear that the spectrum becomes steeper right after $10^{17\,6}$ eV and flattens after $3 \cdot 10^{18}$ eV. The change in the spectral slope forms a dip where a minimum lies between $2 \cdot 10^{18}$ and $5 \cdot 10^{18}$ eV. We divide the spectrum into three energy regions determined by eye and fit them to a power law in each region. Table 1 gives the normalization and slope in each region. Also listed in the table is the overall fit to a single power law . The latter is clearly a poor fit. The expected number of events from the overall fit can be compared to the actual number of events. The comparison of 5936 expected and 5477 observed between $10^{17\,6}$ eV and $10^{19\,6}$ eV gives a deficit of 5.96 sigma. An alternative way of showing the significance is to show the excess of observed events above $10^{18\,5}$. Here we use the normalization and slope from the overall fit up to $10^{18\,5}$ to calculate the expectation. The total observed events are 283 while the expectation is 230, leading to a 3.49 sigma excess.

Table 1. Spectral slopes and normalizations of J(E) ($m^{-2}sr^{-1}s^{-1}$)

Energy range (eV)	Power index	$log(normalization)$	Normalized at
$10^{17.3} - 10^{19.6}$	-3.18 ± 0.01	-29.593	$10^{18}eV$
$10^{17\,3} - 10^{17\,6}$	-3.01 ± 0.06	-29.495	$10^{18}eV$
$10^{17\,6} - 10^{18\,5}$	-3.27 ± 0.02	-29.605	$10^{18}eV$
$10^{18\,5} - 10^{19.6}$	-2.71 ± 0.10	-32.623	$10^{19}eV$

The stereo spectrum shows clear evidence of structure. The structure is consistent with appearance of a new, harder spectrum which dominates the softer component at energies above $5 \cdot 10^{18}$ eV. It is of great interest to ask if the composition of cosmic rays undergoes a change in this energy interval as well.

4.COMPOSITION MEASUREMENT

The position of shower maximum in the atmosphere (X_{max}) in gm/cm^2 is sensitive to the composition of the parent particle. Protons, for instance, will interact more deeply in the atmosphere than heavy nuclei. Air showers produced by protons are also expected to have larger fluctuations than those produced by heavy nuclei. As a result, measuring the distribution of shower X_{max} can be used to infer the primary cosmic ray composition.

5. THE DATA AND MONTE CARLO SIMULATION

We impose the following cuts on the data: $\delta X_{max}/X_{max} \leq 0.12$, minimum viewing angle of pmt tube to track $\geq$ 20 degrees, and energy $\geq$ 0.1 EeV. The first cut removes poorly reconstructed events, the second removes events with strong Cherenkov light contamination and the third insures that the data is above the detector trigger threshold. After cuts, we have 8790 events in the energy range from .1 to 30 EeV and 5129 events from .3 to 30 EeV.

Monte Carlo data is generated by using two different kinds of simulations [Gaisser et al. 1993]. The first simulates the extensive air shower development. Because the nature of the hadronic interactions at these energies is not well known, we use three different hadronic models. The first two are high inelasticity models (QCD Pomeron and QCD minijet) while the third is a low inelasticity statistical model. The parameters of the models are described in [Gaisser et al 1993] in more detail. All three models use the same inelastic total cross-section energy dependence (near log(s)). The models are all good fits to accelerator data for p-p interactions but represent different extrapolations of the behaviour of the fragmentation region to the energy range of interest. Nucleus-air interactions are modelled by following the reinteractions of the beam in the nucleus in a way that is appropriate for each hadronic model. The statistical model leads to a very poor fit to our data for any composition assumption and is hence ruled out. The QCD Pomeron and QCD minijet models result in adequate fits (they differ in their predictions by order of 10 gm/cm^2 whereas, as will be seen below, the position of the X_{max} peak in any given model changes by 80 gm/cm^2 from purely protonic to a purely iron composition). The QDC-Pomeron model gives the best overall fit to the data, hence we will use it alone in the following discussion.

The second simulation takes the generated extensive air shower profile and generates the appropriate scintillation and cherenkov light, propagates the light through the atmosphere and determines which tubes in F.E. I and F.E. II would trigger. For triggered tubes, the program determines the resulting pulse integrals and relative firing times. The program then generates a set of fake events, whose format is identical to the real data. This fake data set is then reconstructed using the same programs that we use for real data.

6. COMPARISON OF DATA WITH MONTE CARLO

We compare the measured X_{max} distributions to expectations for pure Fe and pure proton monte carlo data in four energy bins. Fig. 2 shows data and Fe and pure proton X_{max} simulated data normalized to equal areas. Note that the falling part of the X_{max} distribution (the decrement) depends on the inelastic cross section with air nuclei, hence the proton distribution falls more slowly than iron. The falling slope of the data is consistent with the proton slope but the rise and the peak of the data distribution is the same as predicted for iron, at least in the lower energy bins. The data thus requires a significant admixture of iron or similar heavy nuclei in the lower energy bins. Data in the higher energy bins clearly require a larger admixture of protons while the 3 to 10 EeV bin data can be largely accounted for by protons alone. Detailed fits show that the proportion of protons rises from .21 $\pm$ 0.07 near .3 EeV to .43 $\pm$ 0.04 for events with > 1.0 Eev energy.

7. ELONGATION RATE

The elongation rate is the rate of change of the average depth of shower maximum per decade of shower energy. Fig. 3 shows this dependence for data, pure Fe and pure proton showers using the QCD Pomeron hadronic model. The elongation rate for any pure elemental composition is 50 gm/cm^2 per decade of energy. It follows that a mixed but unchanging composition is also expected to have the same elongation rate. The elongation rate for the data, from 0.1 to 10 EeV is 69$\pm$1.9 gm/cm^2. Examination of the data shows that a single straight line is not a good fit. The elongation rate from 0.3 to 10 EeV is 78.9 $\pm$ 3 gm/cm^2 while the elongation rate below 0.3 EeV is consistent with the expected 50 gm/cm^2. This picture also implies a composition that is growing lighter with energy, going from a heavy composition near 0.3 EeV to a proton dominated composition near 10 EeV.

8. CONSISTENCY OF SPECTRUM AND COMPOSITION DATA

The fact that both the spectrum and the composition of cosmic rays undergo a change near 3 EeV may imply that we are observing a new cosmic ray component emerging from the lower energy flux. To test this

hypothesis, we fit the stereo spectrum to a two component power law. Fig. 5 shows the result of such a fit. The best fit results from $10^{17.6}$ to $10^{19.6}$ are: $log(j(E)(m^{-2}s^{-1}sr^{-1}eV^{-1}) = 33.185 - 3.496 \cdot log(E)$ for the softer energy component and $log(j(E)(m^{-2}s^{-1}sr^{-1}eV^{-1}) = 16.782 - 2.610 \cdot log(E)$ for the harder energy component. If we associate the softer energy component with a predominantly heavy (Fe) composition and the harder energy component with a predominantly light (p) composition, we can predict the ratio of Fe to protons as a function of energy. The ratio can be expressed as: $iron flux/proton flux = (E/10^{18.5}eV)^{-0.887}$.

Given this ratio and the expected elongation rates for Fe and proton showers shown in Fig. 4, we can predict the position of the average X_{max} as a function of energy. The results are shown as the diamonds in Fig. 4. The excellent agreement between this simple two component model which comes from a fit to the spectrum and the composition results which come from the X_{max} distribution supports the conclusion that we have indeed observed a transition between two different spectra.

9. MONOCULAR SPECTRUM

Compared to the stereo data, the monocular data set is much bigger but the time fitting leads to larger geometrical errors and thus a larger energy uncertainty. Fig. 5 shows the total monocular spectrum. Due to limited energy resolution this spectrum does not show the degree of structure found in the stereo data. The best fit to the overall spectrum yields $J(E) = 10^{-29.95}(E/10^{18}eV)^{-3.07 \pm 0.01}m^{-2}s^{-1}eV^{-1}$. The figure shows a flattening of the spectrum above 10^{19} eV. The significance of the flattening based on the spectrum slope and normalization below $10^{19}eV$ is 3.5 σ. The flattening extends for only a decade and appears to steepen after $10^{19.7eV}$. We expect 20.6 events above this energy if the flattened spectrum continues but observe 10. More statistics is needed to resolve this.

An event with an energy of 320 EeV is observed. This well measured event is consistent with expectations for either a proton or an Fe nucleus. Because of its great energy, this event is unlikely to come from a distance of greater than 30 Mpc or to be bent by more than 10 degrees by magnetic fields. No obvious astrophysical sources exist in the resulting error box.

9. DISCUSSION

Taken together, the Fly's Eye results on the cosmic ray energy spectrum and chemical composition strongly suggest a transition near $10^{18.5}$ eV to a new source, most likely of extragalactic origin. The present stereo detector runs out of sensitivity above 10 EeV because of limited aperture. Monocular data suffers from limited energy and X_{max} resolution. It is clearly of great interest to extend the X_{max} and spectrum measurements to this region with high statistics. Confirmation of this result requires a detector with at least an order of magnitude increase in aperture at energies above 10 EeV and similar or better resolution in X_{max}. The High Resolution Fly's Eye (HiRes) detector [Bird et al. 1993d] is presently in the prototype stage. Data from the prototype indicates that a full HiRes detector will have an aperture that is more than adequate to answer these questions. The construction and operation of this detector in the next few years should shed further light on this extremely interesting energy region.

REFERENCES

Baltrusaitis, R.M. *et al.*: 1985, Nucl. Instr. Meth., A240, 410
Bird, D. *et al.*: 1993a, submitted to Ap. J. Bird, D. *et al.*: 1993b, Proc. 23rd ICRC, Vol. 2, 55
Bird, D. *et al.*: 1993c, Proc. 23rd ICRC, Vol. 2, 51
Bird, D. *et al.*: 1993d, Proc. 23rd ICRC, Vol. 2, 458
Chi, X. *et al.*: 1992, J. Phys. G., 18, 539
Gaisser, T.K. *et al.*: 1993, Phys. Rev. D. 47, 1991

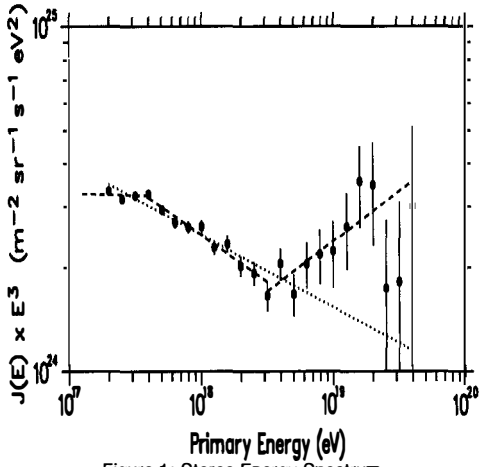

Figure 1: Stereo Energy Spectrum

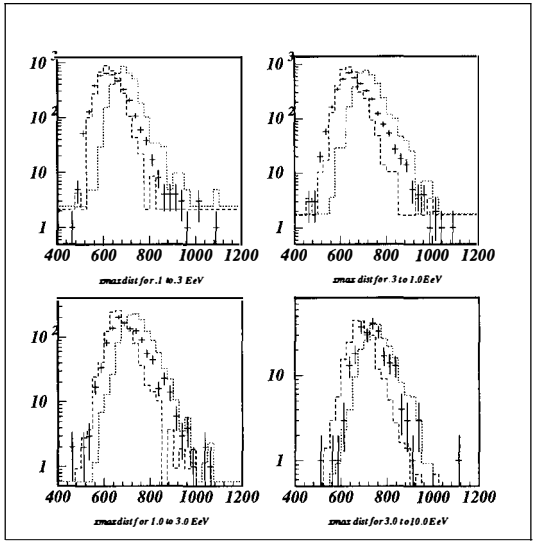

Figure 2: X_{max} distribution for data (crosses), Fe (short dashes) and protons (long dashes) for four energy bins: 0.1 to 0.3 EeV .3 to 1.0 EeV; 1.0 to 3.0 EeV; and 3.0 to 10.0 EeV.

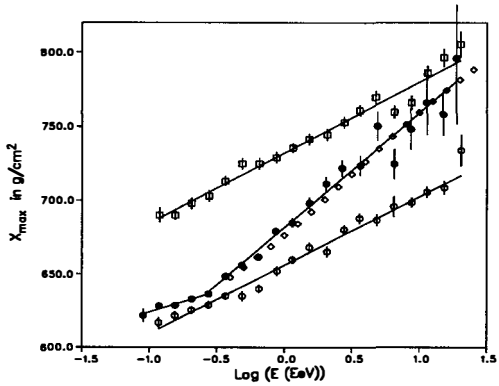

Figure 3: Elongation rate, data (crosses), Fe (stars) and protons(circles). X axis is $log_{10}(E)$. Y axis is X_{max} in gm/cm^2. The error bars indicate the statistical error on the mean.

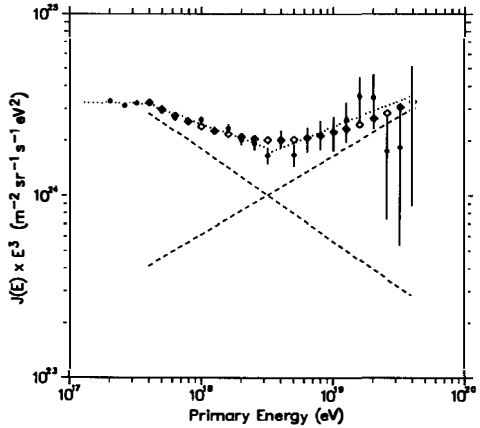

Figure 4: Two Component Fit to Stereo Spectrum

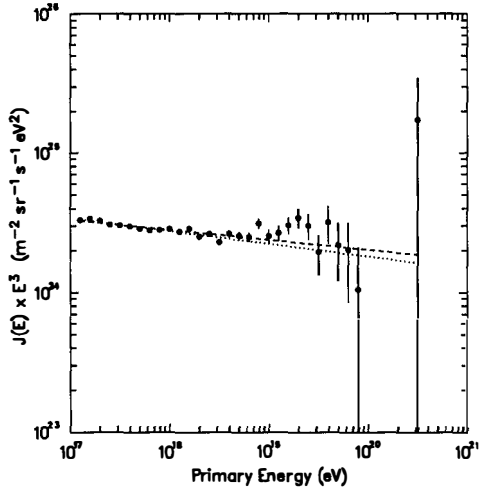

Figure 5: Monocular Energy Spectrum